Analytica Chimica Acta 653 (2009) 109–115

Contents lists available at ScienceDirect

Analytica Chimica Acta

journal homepage: www.elsevier.com/locate/aca

Surface plasmon resonance biosensor based on water-soluble ZnO–Au nanocomposites

Liying Wang[a], Jian Wang[a], Songling Zhang[b], Ying Sun[a], Xiaonan Zhu[a], Yanbo Cao[a], Xinghua Wang[a], Hanqi Zhang[a], Daqian Song[a,*]

[a] College of Chemistry, Jilin University, Qianjin Street 2699, Changchun 130012, PR China
[b] Department of Gynecology and Obstetric, The First Hospital of Jilin University, Xinmin Street 71, Changchun 130021, PR China

ARTICLE INFO

Article history:
Received 6 June 2009
Received in revised form 27 August 2009
Accepted 2 September 2009
Available online 6 September 2009

Keywords:
Wavelength modulation
Surface plasmon resonance
ZnO–Au nanocomposites
Human IgM

ABSTRACT

A wavelength modulation surface plasmon resonance biosensor based on ZnO–Au nanocomposites for the detection of human IgM was developed. Self-assembly technique has the advantages of flexibility, simplicity and the precise control of film component and was applied to the building of the sensor. The ZnO–Au nanocomposites are in a dumbbell-like shape and can be immobilized on the Au film through 1,6-hexanedithiol by covalent attachment. Meanwhile the activated ZnO nanocrystals can be used to connect protein. The biosensor based on ZnO–Au nanocomposites was used to detect human IgM. Some experimental conditions were examined and optimized. In the selected conditions, the modified biosensor exhibits a satisfactory response for human IgM in the concentration range of 0.30–20.00 $\mu g\,mL^{-1}$. However, the biosensor without ZnO–Au nanocomposites shows a response for human IgM in the concentration range of 1.25–20.00 $\mu g\,mL^{-1}$. Compared with the biosensor based on Au film, when the biosensor based on the ZnO–Au nanocomposites was applied, the sensitivity for determination of human IgM is significantly enhanced.

1. Introduction

Surface plasmon resonance (SPR) biosensor is a powerful tool for its versatility and capability in real time monitoring the association or dissociation of biomolecules on the solid/liquid interfaces of the sensor without labeling of the biomolecules [1]. This technique utilizes the evanescent wave of a surface plasmon to detect chemical changes occurring at the surface of a thin metal film such as Au or Ag [2]. Because SPR biosensor provides a rapid, label-free and highly sensitive assay, it is especially suitable for the determination of interactions between biological molecules, such as protein–protein interaction [3], DNA–protein interaction [4], drug–serum albumin interaction [5], drug–liposome interaction [6] and especially antibody–antigen interaction [7]. A number of SPR systems based on various sensing membranes, such as colloidal Au [8], Ag [9], magnetical microbead [10,11] and TiO_2 film [12], were applied.

One of the most critical points in the development for high quality of biosensors is the effective and controlled immobilization of the appropriate proteins on the surface of the biosensor. Recently metal nanoparticles on the surface of semiconductor nanostructures have become a popular research topic because of the improved optical properties of the semiconductor [13–15]. The couplings of metal and semiconductor were expected to change the optical and electronic properties. It has been reported that the SPR electron and energy transfer from the metal surface to the surrounding semiconductor materials significantly modify the optical properties of the metal and the semiconductor [16,17].

Au nanoparticle has been used widely in immunoassays owing to its excellent properties, such as easy reductive preparation, water-solubility, high chemical stability, significant biocompatibility and affinity [18]. Moreover, it has also been known that thiol terminal groups are able to bind stably to the Au surface as the formation of monolayer which is driven by a strong, specific interaction between the thiol and the Au surface. ZnO nanocrystals can achieve higher sensitivity and efficiency due to the increase of surface area to volume ratio, which are beneficial to light absorption/emission or electron transfer [19]. Generally, ZnO nanocrystals are synthesized in organic media and unstable in aqueous solution, while biological conjugation usually exists in water solution. In order to satisfy the primary requirement of biological research, the surface of ZnO nanocrystals should be modified. ZnO–Au nanocomposites could be applied in immunoassays for their characters such as high solubility in water, biocompatibility and lower toxicity than

* Corresponding author. Tel.: +86 431 85168399; fax: +86 431 85112355.
E-mail address: songdq@jlu.edu.cn (D. Song).

0003-2670/$ – see front matter © 2009 Elsevier B.V. All rights reserved.
doi:10.1016/j.aca.2009.09.001

other semiconductor nanocrystals. Recently, several methods for preparing dumbbell-like structure ZnO–Au hybrid nanocomposites were studied. Wang et al. used ZnO nanocrystals as seeding material for nucleation and then growth of reduced gold by citrate to form the water-soluble ZnO–Au nanocomposites [16]. Lee et al. successfully synthesized Au–ZnO nanocomposites through the nucleation and decomposition of zinc hydroxide at the surface of Au nanoparticle which is used as seeding material and reduced by $NaBH_4$ [19]. Compared with the toxic Cd element semiconductor nanocrystals, ZnO–Au hybrid nanocomposites have evident advantages, such as biologically nontoxic, good biocompatibility and higher chemical stability, so they have potential applications in biological technology studies [20]. A novel method for identifying DNA microarrays based on ZnO–Au nanocomposites functionalized with thiol-oligonucleotide as probes was described recently [21].

The monolayer and multilayer molecular assemblies at solid surfaces provide the routine approaches for the fabrication of interfaces with well-defined structure, composition and thickness [22]. Multilayer assemblies have been widely applied in areas of chemical and biological sensors.

In this paper, ZnO nanocrystals were prepared as seeding material and then water soluble ZnO–Au nanocomposites with dumbbell-like shape were successfully synthesized [16,23]. The ZnO–Au nanocomposites could provide organic functionality for bioconjugation and then application in SPR biosensor. In order to build a biosensor based on ZnO–Au nanocomposites, it is critical to study the attachment mechanism of the protein onto the ZnO–Au surface, and the interaction between the surface and the biomaterials. The thiol–gold interaction was relatively easy, which was applied to the self-assembly of monolayer (SAM) on Au surface. As 1,6-hexanedithiol (HDT) is a disulfide compound, it could be used to connect Au film and the ZnO–Au nanocomposites. The reactive ZnO surface offers the opportunity for effective bio-ZnO interfaces. First, the ZnO surface could be hydroxylized readily in water, followed by silanization with 3-aminopropyltrimethoxysilane (APTS). Then the gluteraldehyde was used as the bridge to bind the protein and silanized ZnO. As a result, the immobilization of protein on the surface of the ZnO–Au sensor is achieved. The binding of protein–protein leads to changes in the refractive index at the sensor surface, which results in the shifts of resonant wavelength that can be easily measured by SPR biosensor.

IgM is large (950 kDa) pentamer formed by five IgG-like monomers connected through a polypeptide chain rich in disulfide bonds and characterized by the presence of a disulfide-rich J chain [24]. IgM normally constitutes about 10% of serum immunoglobulins and IgM antibody is prominent in early immune responses to most antigens and largely confined to plasma due to its large size.

2. Experimental

2.1. Reagents

Human IgM and goat anti-human IgM were purchased from Beijing Boisynthesis Biotechnology Company. Bovine serum albumin (BSA) was purchased from Ding Guo Biotechnology Company (Beijing, China). 3-Aminopropyltrimethoxysilane (APTS), 3-mercaptopropionic acid (MPA) and 1,6-hexanedithiol (HDT) were purchased from Jkchemical. Hydrogen tetrachloroauratehydrate, trisodium citrate, gluteraldehyde, zinc acetate dehydrate, lithium hydroxide monohydrate, ethanol and all other chemicals were of analytical reagent grade. All solutions were prepared with ultra pure water. Human IgM and goat anti-human IgM were stored at −20 °C. Sodium phosphate buffered saline (PBS, 0.01 mol L^{-1}, pH 7.4) was used as running buffer.

2.2. Equipment

The wavelength modulation SPR biosensor installed in our laboratory was used. It is working with Kretschmann configuration to achieve the resonant condition by attenuated total reflection (ATR) in a prism. A K9 glass slide was used whose diameter and thickness were 12 and 0.7 mm, respectively. A 2 nm adhesive layer of Cr followed by a 50 nm layer of Au was deposited on the glass slide, then the glass slide with Au film was put on base of a prism (K9 glass) using a suitable index matching oil (cedar oil). A halogen tungsten lamp is used as the excitation light source in conjunction with a constant voltage transformer. The light from this source passes through a polarizer and two lenses and becomes TM-polarized parallel light. The parallel polychromatic light beam passes through the optical prism and excites surface plasmon at the interface between the Au film and the analyte. The output light is guided into the optical fiber and then enters the full wave length spectrophotometer (Ocean Optics, Inc., USA). A 2048 element linear array charge-coupled device (CCD) was used as the detector. A 100 μL volume flow cell was used. The interaction between the analyte in the solution and the biomolecular element immobilized on the SPR biosensor produces a change in refractive index (RI) profile that is observed as a shift in the SPR resonant wavelength. The surface plasmon resonance manifests itself on a characteristic dip in the wavelength dependence on the intensity of reflected light and the intensity of reflected light is minimum at the resonant wavelength.

2.3. Procedures

2.3.1. Preparation of water-soluble ZnO–Au nanocomposites

Water-soluble ZnO–Au nanocomposites were prepared as followed [16,23]. Briefly, 50 mL of ethanol containing 1.10 g zinc acetate dihydrate was refluxed while stirring at about 80 °C for 100 min and the precursor solution was obtained. Then the precursor was hydrolyzed by adding 50 mL of ethanol containing 0.29 g lithium hydroxide monohydrate in an ultrasonic bath at 0 °C for 30 min.

The resulting in 6 mL of ZnO nanocrystals solution was precipitated by adding 25 mL of 0.15 mmol L^{-1} trisodium citrate solution. The obtained precipitated ZnO nanocrystals by centrifugation were redispersed in 30 mL of 3.0 mmol L^{-1} trisodium citrate solution with the aid of ultrasonic, and then 20 mL of 0.5 mmol L^{-1} $HAuCl_4$ solution was added while vigorously stirring at room temperature. During vigorous stirring for at least 48 h, these hydrophobic ZnO nanocrystals were transformed into water-soluble ZnO–Au nanocomposites gradually [16]. The color of the solution changed from pale yellow to purple. These ZnO–Au nanocomposites homogeneously dispersed in aqueous solution.

2.3.2. The modification of Au film

The glass slide with Au film was immersed into ethanol/water solution (v/v, 2:1) containing the HDT at the concentration of 10 mmol L^{-1} for 24 h. Then, Au film was rinsed several times with ethanol and ultra pure water, and dried with gaseous nitrogen. After the immobilization of HDT, the glass slide was immersed into water-soluble ZnO–Au nanocomposites solution for 12 h. Then, it was rinsed with ultra pure water, and dried with gaseous nitrogen.

The silanization process of the ZnO–Au film was completed with 3-aminopropyltrimethoxysilane (APTS) in ethanol solution (v/v, 4/100) at room temperature for 4 h. The alkylamininosilanederivatized surface was rinsed in ethanol for 1–2 min, washed in ultra pure water. The silanized ZnO–Au film was treated with 2 mL of 2% gluteraldehyde solution in PBS for 4 h. The modified ZnO–Au film was rinsed thoroughly with ultra pure water to remove the excess gluteraldehyde, and then dried with gaseous nitrogen.

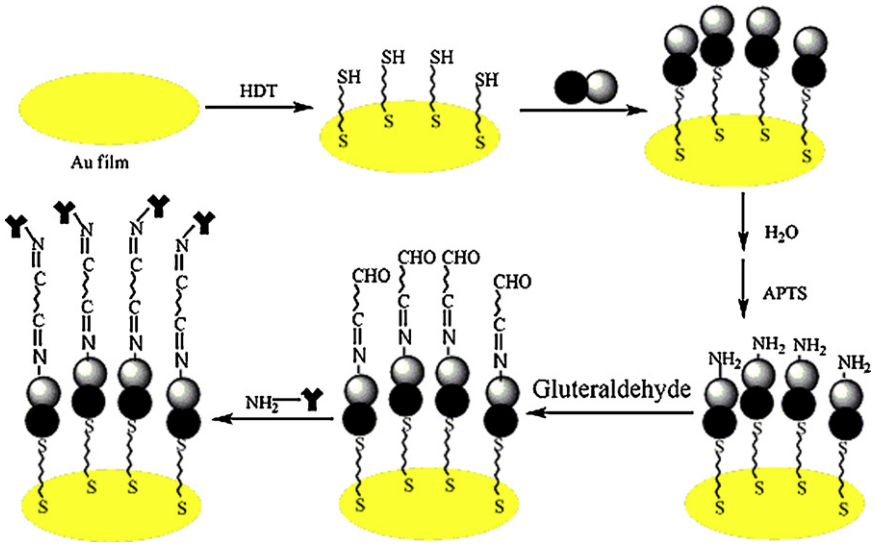

Fig. 1. A schematic diagram of the immobilization of antibody on the surface of the Au film. (●) Au nanoparticles, (◐) ZnO nanocrystal, (●◐) ZnO–Au nanocomposites.

2.3.3. Protein immobilization procedure

The glass slide with modified Au film was fixed under the flow cell. Deionized water was first injected into the flow cell. Then PBS was injected into the flow cell as the baseline solution and goat anti-human IgM was injected into the flow cell to covalently attach to the aldehyde-activated surfaces. After 12 h, PBS buffer was injected into the flow cell to wash off noncovalently bound antibody and to stabilize the baseline. Prior to the analysis, 1 mol L^{-1} ethanolamine hydrochloride (pH 8.0) was used to block the non-specific binding sites on the biosensor surface for 10 min. A schematic diagram of the immobilization of antibody on the surface of the Au film is shown in Fig. 1.

As a contrast, the glass slide with Au film was also fixed under the flow cell. After PBS was injected into the flow cell as the baseline solution, 10 mmol L-1 MPA was injected into the flow cell. Then —COOH group was activated with NHS under the catalysis of EDC for 20 min, goat anti-human IgM was injected into the flow cell. The next procedures were the same as that mentioned above.

2.3.4. Immunoassay

At room temperature, different concentrations of human IgM diluted with PBS buffer were separately injected into the flow cell over the immobilized antibody surface prepared and shifts of the resonant wavelength ($\Delta\lambda$) were measured as time prolonged. PBS buffer was injected over the surface to monitor the dissociation of antigen from antibody for 30 min. Due to a large amount of ions in the PBS buffer, the antigen could be washed by impulse injection of PBS buffer [25]. When the antigen was dissociated from the antibody on biosensor surface, the SPR resonant wavelength returned to the baseline and another sample was injected into the flow cell.

3. Results and discussion

3.1. Morphology of ZnO–Au nanocomposites

The morphology of ZnO–Au nanocomposites was characterized by transmission electron microscopy (TEM) and the experimental result is shown in Fig. 2. The molar ratio of ZnO to $HAuCl_4$ is 30:1 and an excess of ZnO nanocrystals are required. It can be seen from Fig. 2 that ZnO–Au nanocomposites have dumbbell-like structure and appear very dark. The average size of the ZnO–Au nanocomposites was about 10 nm. The bare ZnO nanocrystals were unstable in aqueous solution and they will be precipitated when adding water due to the weak interaction of surface ligand and water [21]. While, after the linking with Au nanoparticle, ZnO–Au nanocomposites were stable in aqueous phase which further confirmed that ZnO–Au nanocomposites were synthesized successfully.

3.2. Optical properties of ZnO–Au nanocomposites

The optical properties of ZnO–Au nanocomposites were characterized by UV–visible absorption and photoluminescence (PL) spectrometry, respectively. Fig. 3 shows the UV–vis absorption spectra of pure ZnO nanocrystals (a) and the ZnO–Au nanocomposites (b). The absorption peak, around 330 nm, exhibits well-defined exciton band of ZnO nanocrystals. This is the most distinctive absorption peak of semiconductor, which is the mainly characteristic difference from metal. Fig. 3(c) shows the absorption spectrum for Au nanoparticles and the inset of Fig. 3(d) shows the absorption spectrum for ZnO–Au nanocomposites. The absorption of Au nanoparticles and ZnO–Au nanocomposites in water are centered at 520 nm and 546 nm, respectively. The distinctly broadened and red-shift of the surface plasmon spectra of the ZnO–Au nanocomposites could be observed clearly. The reason is that the strong interfacial coupling between Au and ZnO results in electrons transfer from Au to ZnO during the formation of ZnO–Au nanocomposites [16].

Fig. 4 shows the PL spectra of ZnO nanocrystals and the ZnO–Au nanocomposites. The PL spectra are composed of two emission bands in the UV–visible range. The UV emission band centered at 365 nm is ascribed to the radiative recombination, which occurs due to recombination between the electrons in a conduction band and the holes in a valence band. The visible range emission band centered at 520 nm is ascribed to the nonradiative recombination, which occurs due to the recombination between the electrons in a deep defect level or a shallow surface defect level and the holes in a valence band [26,27]. ZnO–Au nanocomposites exhibit UV emission at 365 nm and weaker visible emission at about 520 nm than that of pure ZnO nanocrystals. When Au nanoparticles combined with ZnO, the electrons accumulate at the interface between Au and ZnO, which leads to the electron transfer from the Au nanoparticles to the ZnO side.

3.3. Preparation of SPR biosensor based on ZnO–Au nanocomposites

Traditionally, the SPR sensor chip surface is usually coated with monolayer as a thin hydrogel matrix or sulfhydryl compound. The

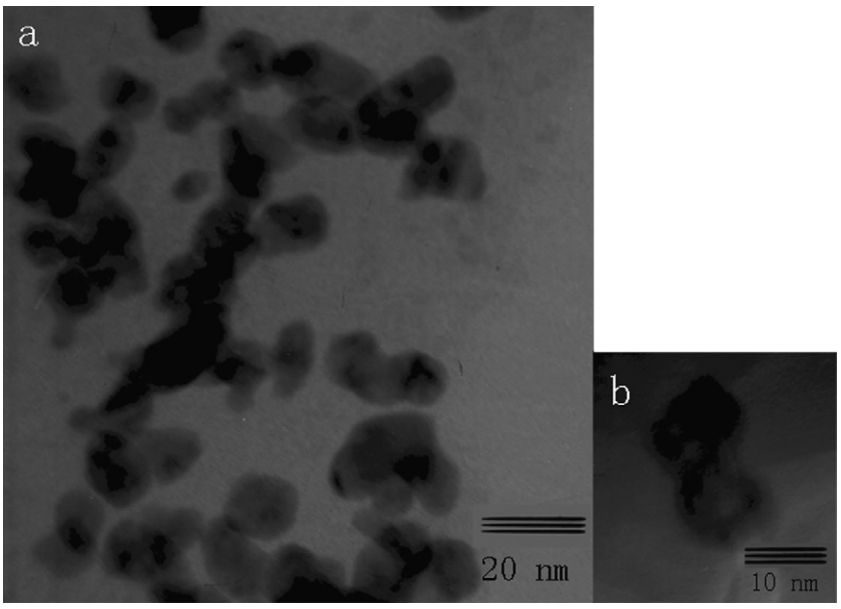

Fig. 2. Transmission electron microscopy (TEM) image of ZnO–Au nanocomposites.

receptor molecules were covalently immobilized on the monolayer for specific analyte capture. Complex formation with ligands leads to a change in the refractive index, which can be monitored in real time. Here a new SPR biosensor is constructed based on ZnO–Au nanocomposites.

The water-soluble ZnO–Au nanocomposites with dumbbell-like shape provide dual functionality. As HDT is a disulfide compound, Au nanoparticles can be successfully immobilized on Au film through the thiol groups stably. ZnO nanocrystals can be used to connect protein by the virtue of its characteristic functional properties. Before the immobilization of protein on ZnO, a hydroxylation step was required. The ZnO surface has a high density of unsaturated bonds, which could be hydroxylized readily upon the contact with ultra pure water [28,29]. In the next step, APTS acts as a bridge which is bound to gluteraldehyde. After the silanization process, the modified Au film changes from hydrophobicity to hydrophilicity which indicated that the terminal amino group in APTS is bound stably on the biosensor surface. Then covalent multilayer can be assembled on Au film and terminal aldehyde groups on the surface could bind to goat anti-human IgM.

After the ZnO–Au nanocomposites were immobilized and activated on the Au film, the glass slide modified was fixed under the flow cell. When PBS was injected into the flow cell as the baseline solution, a red-shift of the resonant wavelength for the sensor based on ZnO–Au nanocomposites can be observed. The shift of resonant wavelength for the sensor based on ZnO–Au nanocomposites was about 30 nm compared with that for the sensor based on Au film, which was modified by MPA. The couplings of Au nanoparticle and ZnO nanocrystals result in the energy transfer from the metal surface to the surrounding semiconductor materials and induce the change of the optical and electronic properties. Meanwhile, the change of the thickness of the SPR biosensor film due to layered assemblies was responsible for the red-shift of the resonant wavelength. And the shift of resonant wavelength towards long wavelength could increase the sensitivity of the sensor in wavelength modulation SPR biosensor [1].

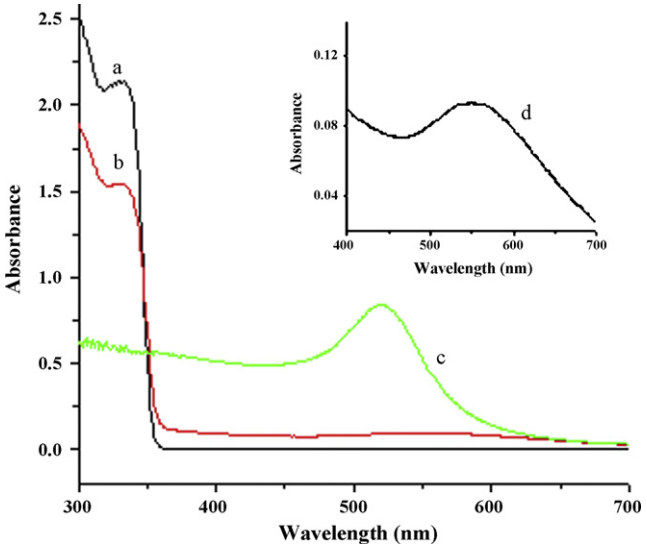

Fig. 3. Optical absorption spectra of ZnO nanocrystals (a), ZnO–Au nanocomposites (b) and Au nanoparticles (c). *Inset*: the surface plasmon absorption band corresponding to Au nanoparticles in ZnO–Au nanocomposites (d).

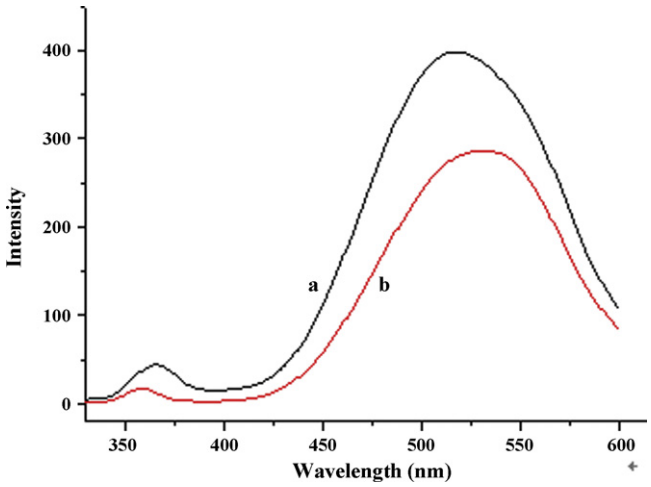

Fig. 4. Photoluminescence spectrometry of ZnO nanocrystals (a) and ZnO–Au nanocomposites (b).

3.4. Immobilization of goat anti-human IgM

After the Au film with ZnO–Au nanocomposites was activated, goat anti-human IgM at different concentrations was separately injected into the flow cell to perform its binding on the activated surface. The terminal aldehyde group of gluteraldehyde can be bound with the amine group of the antibody to form Schiff bases easily. The ZnO–Au nanocomposites have a dual function. Au nanoparticles can be successfully immobilized on Au film through the thiol groups and act as a binding agent for the ZnO nanocrystals. The activated ZnO nanocrystals effectively connect with antibody through covalent attachment. The kinetic adsorption curves of antibody at different concentrations on the sensor surface based on ZnO–Au nanocomposites are shown in Fig. 5. It can be seen from Fig. 5 that the terminal aldehyde group of gluteraldehyde has a strong response to antibody and the antibody could be immobilized steadily on the biosensor surface. In theory, the protein can be adsorbed directly on the Au nanoparticles, while the adsorption is hardly to achieve in this paper. Before the protein injected into the flow cell, multilayer films have been constructed on the layer of Au nanoparticles, so that the protein is hard to attach Au nanoparticles directly. In addition, the attachment between Au nanoparticles and protein is weaker compared with covalent attachment between aldehyde group and protein. When PBS buffer was injected into the flow cell, almost no change in resonant wavelength was observed. The result indicated that there is no non-specific attachment in the process of antibody immobilization and Au nanoparticle does not participate in the protein adsorption. Here the Au nanoparticle simply acts as a binding agent for the ZnO nanocrystals. Then, 1 mol L^{-1} ethanolamine hydrochloride (pH 8.0) was used to block the non-specific binding sites on the biosensor surface.

The effects of the different concentrations of goat anti-human IgM on the shifts of the resonant wavelength are also shown in Fig. 5. It can be seen that the resonant wavelength shows evident shift at first and then changes slowly with the time increase. A sensing layer composed of immobilized antibody formed well on the sensing film. Due to the increase of the conjugates concentration, more antibodies were immobilized on the sensor surface. While with the increase of the concentration of goat anti-human IgM, the antibody immobilized on surface reaches saturation, which results in no change of the resonant wavelength. As a result, 25 μg mL^{-1} was chosen as the optimum concentration of goat anti-human IgM for the detection of human IgM.

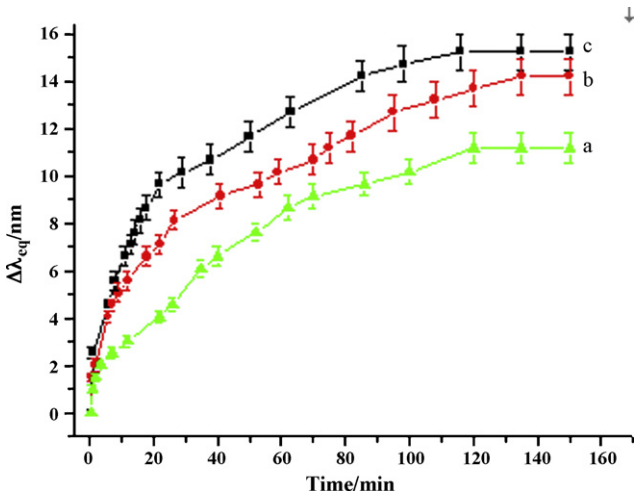

Fig. 5. Kinetic adsorption curves of goat anti-human IgM on ZnO–Au nanocomposites. The concentration of goat anti-human IgM: (a) 10 μg mL^{-1}, (b) 25 μg mL^{-1} and (c) 50 μg mL^{-1}.

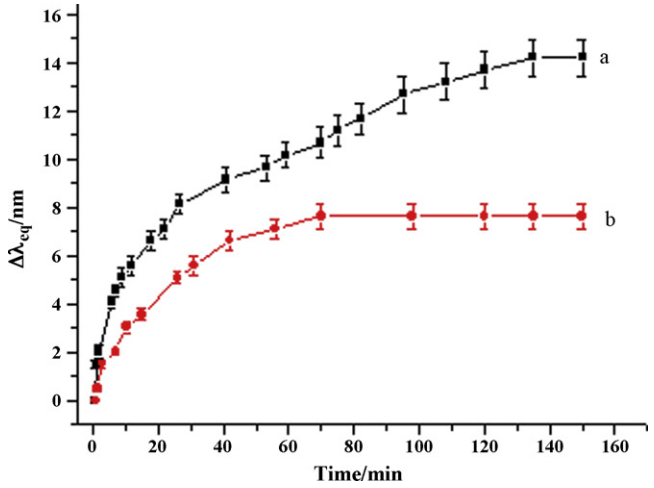

Fig. 6. Kinetic adsorption curves of goat anti-human IgM at concentration of 25 μg mL^{-1} on the sensor based on ZnO–Au nanocomposites (a) and the sensor based on Au film (b).

As shown in Fig. 6(a), when the concentration of goat anti-human IgM is 25 μg mL^{-1}, a sensing layer composed of immobilized antibody formed well on the sensor surface. The covalent attachment between the amine group and the aldehyde group is a good stratagem for the immobilization of antibody on the Au film [7]. It can be seen from Fig. 6(a) that the shift of the resonant wavelength is fast at first and then slow and reached about 75% of its total shift within 1 h. The maximum resonant wavelength shift for the immobilization of goat anti-human IgM is 14.22 nm for the sensor based on ZnO–Au nanocomposites within 150 min which is favor for forming the sensing film firmly. As a contrast, 25 μg mL^{-1} goat anti-human IgM was also immobilized on the Au film to detect human IgM. It can be seen from Fig. 6(b) that a sensing layer composed of immobilized antibody formed well on the sensor surface and the maximum resonant wavelength shift for immobilization of goat anti-human IgM is 7.63 nm within 150 min for sensor based on Au film. Due to the ZnO/Au nanocomposites on the biosensor surface, the binding sites would be increased. It can be seen from the results that the maximum resonant wavelength shift based on ZnO/Au nanocomposites was about two times than that based on Au film. The biosensor extended the application of ZnO/Au nanocomposites in immunoassay. When the biosensor based on ZnO/Au nanocomposites were used, the sensitivity has a modest increase over a conventional biosensor based on Au film.

3.5. Determination of human IgM

At room temperature, after the goat anti-human IgM was immobilized on the surface of the biosensor, human IgM at different concentrations was separately injected into the flow cell. The shifts of resonant wavelength due to antibody–antigen immunoreaction were measured. The SPR response of the adsorption and the dissociation of human IgM can be monitored in real time. Fig. 7 shows the relationship between the shifts in the resonant wavelength and the concentrations of human IgM. It can be seen that the SPR biosensor based on ZnO–Au nanocomposites shows a satisfactory response to human IgM in the concentration range of 0.30–20.00 μg mL^{-1}. The minimum shift of resonant wavelength is 0.51 nm at 0.30 μg mL^{-1} and the maximum shift of resonant wavelength is 7.53 nm at 20.00 μg mL^{-1}. The SPR biosensor based on Au film shows a response to human IgM in the concentration range of 1.25–20.00 μg mL^{-1}. The minimum shift of resonant wavelength is 0.51 nm at 1.25 μg mL^{-1} and the maximum shift of resonant wavelength is 4.10 nm at 20.00 μg mL^{-1}. The results indicate that the SPR

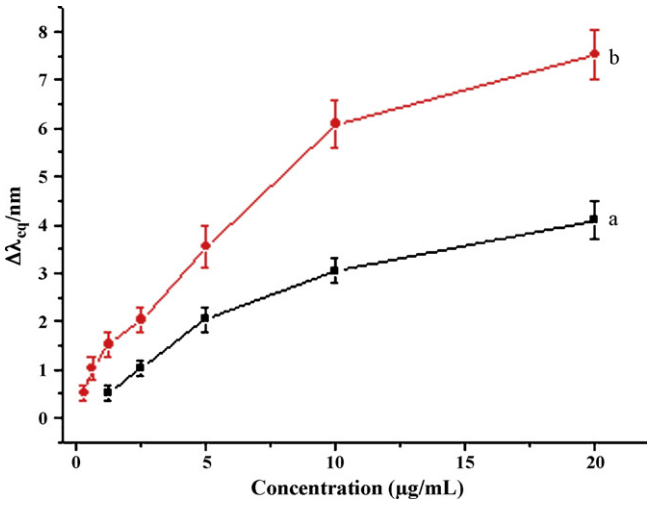

Fig. 7. The relationship between the concentration of human IgM and the shifts in the resonant wavelength. (a) The sensor based on Au film and (b) the sensor based on ZnO–Au nanocomposites.

biosensor based on ZnO–Au nanocomposites is suitable for detecting of human IgM. With the increase of concentration of human IgM, the binding sites of the antibody immobilized on the surface will be saturated. When the concentration of the human IgM increased, no obvious shift of the resonant wavelength was observed and then this concentration is the upper detection limits. The detected minimum resonant wavelength shift of the SPR biosensor installed in our laboratory is 0.51 nm, and the lower detection limits of the antigen are determined by the minimum shift of resonant wavelength.

When Au nanoparticles are combined with ZnO nanocrystals, the electron transfer between Au and ZnO occurred and the optical and electronic properties changed. In the ZnO–Au nanocomposites, the localized electromagnetic effect of the Au surface plasmon is mostly responsible for the shift of resonant wavelength. The surface plasmon of the Au nanoparticles might be resonantly excited through energy transfer in the near field and create a stronger local electromagnetic field [14,30]. The incident light field coupling to the local surface plasmon field might induce stronger localized electromagnetic field in the ZnO–Au nanocomposites, which further enhances the shift of resonant wavelength. On the other hand, when the ZnO–Au nanocomposites were used, the thickness of the sensing membrane increases and the resonant wavelength moves to longer wavelength, which results in the sensitivity enhancement of the wavelength-modulation SPR biosensor.

The evaluation of the non-specific binding interaction was performed by detecting rabbit IgG and BSA. After the goat anti-human IgM was immobilized on the surface of the biosensor, rabbit IgG and BSA at the concentrations of 10 μg mL^{-1} were separately injected into the flow cell for 30 min. There were no observable shifts of the resonant wavelength, which indicated the selective binding of human IgM.

3.6. Calculation of binding constant K_A

For a 1:1 reaction of antigen (Ag) and antibody (Ab), Ag + Ab = AgAb, the binding constant is K_A:

$$K_A = \frac{[AgAb]}{[Ag][Ab]} \quad (1)$$

The association phase of the interaction kinetics measured as SPR signal can be expressed [31–33]:

$$\frac{d\Delta\lambda}{dt} = k_a[Ag](\Delta\lambda_{max} - \Delta\lambda) - k_d\Delta\lambda \quad (2)$$

where $d\Delta\lambda/dt$ is the rate of the change of SPR response, [AgAb] is corresponding to the SPR biosensor signal at equilibrium, [Ag] is the concentration of antigen in the solution, [Ab] is corresponding to $(\Delta\lambda_{max} - \Delta\lambda_{eq})$, k_a and k_d are association and dissociation rate constants, respectively. $\Delta\lambda_{max}$ is the SPR response corresponding the maximum capacity of binding antigen on the sensor surface. $\Delta\lambda$ is the bound antigen measured as the biosensor response at time t. At equilibrium, $\Delta\lambda$ should be expressed as $\Delta\lambda_{eq}$, and $d\Delta\lambda_{eq}/dt = 0$. According to $K_A = k_a/k_d$, Eq. (2) becomes:

$$\frac{\Delta\lambda_{eq}}{[Ag]} = K_A\Delta\lambda_{max} - K_A\Delta\lambda_{eq} \quad (3)$$

$\Delta\lambda_{eq}$ is the bound antigen measured as the biosensor response at equilibrium. [Ag] is the concentration of antigen in the solution. The relationship between the $\Delta\lambda_{eq}$ and [Ag] has been shown in Fig. 7. To a particular type of biosensor $\Delta\lambda_{max}$ is a fixed value. A plot of $\Delta\lambda_{eq}/[Ag]$ against $\Delta\lambda_{eq}$ can be used to obtained K_A from the slope of the plot. The binding constant K_A for human IgM is 1.68×10^8 L mol^{-1}.

4. Conclusion

The detection of human IgM with the wavelength modulation SPR biosensor based on ZnO–Au nanocomposites was presented. The shape and the average size of the ZnO–Au nanocomposites were measured by TEM. The activated ZnO surface offers the opportunity for effective connect with antibody. A series of immunoassay with different concentrations of goat anti-human IgM were conducted and the results indicate that 25 μg mL^{-1} is the optimum concentration for the detection of human IgM. When the concentration of goat anti-human IgM is 25 μg mL^{-1}, the biosensor based on ZnO–Au nanocomposites exhibits a response in the concentration range of 0.30–20.00 μg mL^{-1}. And the lowest concentration that could be detected is lower than that based on the Au film. Therefore, the biosensor based on ZnO–Au nanocomposites shows high sensitive and is suitable for the detection of human IgM.

Acknowledgements

This work was supported by National Natural Science Foundation of China (No. 20727003) and Science and Technology Developing Foundation of Jilin Province (No. 20070551).

References

[1] J. Homola, S.S. Yee, G. Gauglitz, Sens. Actuators B 54 (1999) 3.
[2] X. Liu, Y. Sun, D.Q. Song, Q.L. Zhang, Y. Tian, S.Y. Bi, H.Q. Zhang, Anal. Biochem. 333 (2004) 99.
[3] T. Fujino, Y. Sato, M. Une, T. Kanayasu-Toyoda, T. Yamaguchi, K. Shudo, K. Inoue, T. Nishimaki-Mogami, J. Steroid, Biochem. Mol. Biol. 87 (2003) 247.
[4] V. Hegde, M. Wang, W.A. Deutsch, DNA Repair 3 (2004) 121.
[5] R.L. Rich, Y.S.N. Day, T.A. Morton, D.G. Myszka, Anal. Biochem. 296 (2001) 197.
[6] E. Danelian, A. Karlén, R. Karlsson, S. Winiwarter, A. Hansson, S. Löfås, H. Lennernäs, M.D. Hämäläinen, J. Med. Chem. 43 (2000) 2083.
[7] S.F. Chou, W.L. Hsu, J.M. Hwang, C.Y. Chen, Biosens. Bioelectron. 19 (2004) 999.
[8] L.A. Lyon, M.D. Musick, M.J. Natan, Anal. Chem. 70 (1998) 5177.
[9] L.Y. Wang, Y. Sun, J. Wang, X.N. Zhu, F. Jia, Y.B. Cao, X.H. Wang, H.Q. Zhang, D.Q. Song, Talanta 78 (2009) 265.
[10] Y. Sun, Y.P. Bai, D.Q. Song, X.Z. Li, L.Y. Wang, H.Q. Zhang, Biosens. Bioelectron. 23 (2007) 473.
[11] Y. Sun, N. Bi, D.Q. Song, Y. Bai, L.Y. Wang, H.Q. Zhang, Anal. Chim. Acta 624 (2008) 294.
[12] M.G. Manera, G. Leo, M.L. Curri, P.D. Cozzoli, R. Rella, P. Siciliano, A. Agostiano, L. Vasanelli, Sens. Actuators B 100 (2004) 75.
[13] M. Fukusima, N. Managaki, M. Fujii, H. Yanagi, S. Hayashi, J. Appl. Phys. 98 (2005) 024316.
[14] K. Okamoto, I. Niki, A. Shvartser, Y. Narukawa, T. Mukai, A. Scherer, Nat. Mater. 3 (2004) 601.
[15] N.E. Hecker, R.A. Höfel, N. Sawaki, T. Maier, G. Stasser, Appl. Phys. Lett. 75 (1999) 1577.
[16] X. Wang, X. Kong, Y. Yu, H. Zhang, J. Phys. Chem. C 111 (2007) 3836.

[17] G.H. Ma, J. He, K. Rajiv, S.H. Tang, Y. Yang, M. Nogami, Appl. Phys. Lett. 84 (2004) 4684.
[18] M.C. Daniel, D. Astruc, Chem. Rev. 104 (2004) 293.
[19] M.K. Lee, T.G. Kim, W. Kim, Y.M. Sung, J. Phys. Chem. C 112 (2008) 10079.
[20] W.Q. Zhang, Y. Lu, T.K. Zhang, W.P. Xu, M. Zhang, S.H. Yu, J. Phys. Chem. C 112 (2008) 19872.
[21] Y.C. Liu, M.Y. Zhong, G.Y. Shan, Y.J. Li, B.Q. Huang, G.L. Yang, J. Phys. Chem. B 112 (2008) 6484.
[22] P. Kohli, G.J. Blanchard, Langmuir 16 (2000) 8518.
[23] G.Y. Shan, M.Y. Zhong, S. Wang, Y.J. Li, Y.C. Liu, J. Colloid Interface Sci. 326 (2008) 392.
[24] M. Caiazzo, A. Alessandrini, P. Facci, Appl. Mater. Interfaces 1 (2009) 514.
[25] R. Pei, X. Cui, X. Yang, E. Wang, Talanta 53 (2000) 481.
[26] J. Yguerabide, E.E. Yguerabide, Anal. Biochem. 262 (1998) 137.
[27] K. Vanheusden, W.L. Warren, C.H. Seager, D.R. Tallant, J.A. Voigt, B.E. Gnade, J. Appl. Phys. 79 (1996) 7983.
[28] S. Krishnamoorthy, T. Bei, E. Zoumakis, G.P. Chrousos, A.A. Iliadis, Biosens. Bioelectron. 22 (2006) 707.
[29] S. Krishnamoorthy, A.A. Iliadis, T. Bei, G.P. Chrousos, Biosens. Bioelectron. 24 (2008) 313.
[30] J.H. Song, T. Atay, S. Shi, H. Urabe, A.V. Nurmkko, Nano Lett. 5 (2005) 1557.
[31] X. Liu, J.Y. Wei, D.Q. Song, Z.W. Zhang, H.Q. Zhang, Anal. Biochem. 314 (2003) 301.
[32] Y. Sun, X. Liu, D.Q. Song, Y. Tian, S.Y. Bi, H.Q. Zhang, Anal. Chim. Acta 569 (2006) 21.
[33] Y. Sun, X. Liu, D.Q. Song, Y. Tian, S.Y. Bi, H.Q. Zhang, Sens. Actuators B 122 (2007) 469.